

Space Vector Based Analysis of the Variation and Control of the Neutral Point Potential of Hysteresis Current Controlled Three-Phase/Switch/Level PWM Rectifier Systems

JOHANN W. KOLAR, UWE DROFENIK, FRANZ C. ZACH

Technical University Vienna, Power Electronics Section 359.5
Gusshausstraße 27, Vienna A-1040, Austria/Europe
Tel.: +43-1-58801-3728 Fax.: +43-1-504 24 77

Abstract

This paper treats the control of the the capacitive output voltage center point of a unidirectional three-phase three-level PWM rectifier system. It is shown that for hysteresis control of the input phase currents and resistive fundamental mains behavior the center point potential can be controlled by an offset of the phase current reference values. Based on the results of a digital simulation the transfer function is determined which describes the dynamic behavior of the system part to be controlled. Furthermore, the dimensioning of the center point voltage control is discussed. There, the considerations are related to an application of the PWM rectifier system for supplying the DC link of an uninterruptible power supply (UPS; rated power: 8 kW). Finally, the control behavior for stationary operation and for a step change of the load of the output voltage center point is examined for verifying the controller dimensioning.

1 Introduction

As described in [1] and [2], unidirectional three-phase three-level PWM rectifiers (cf. Fig.1) show especially the following advantages as compared to conventional two-level converter systems:

- lower harmonic level of the mains currents
- lower blocking voltage stress on the power semiconductor devices
- high reliability being inherent to the systems.

Therefore, three-level PWM rectifiers are of special interest for developing of converter concepts with low effect on the mains. Due to the inclusion of the capacitive center point of the output voltage into the system function we have to provide a control of the potential of the output voltage center point (or a symmetrization of the output partial voltages) for three-level rectifier systems, however. This is to be seen besides the control of the output voltage and the inner-loop control of the mains phase currents as being also required for two-level PWM rectifiers. The possibility of influencing the center point potential is based on the existence of identical switching states concerning the voltage space vector generated at the input of the rectifier system (cf. [3], p.48). These redundant switching states are characterized by opposite loading of the center point (opposite signs of the center point current). This makes possible the control of the center point voltage ideally independent of the current control which determines the rectifier input voltage space vector which has to be generated over a pulse period. In general one has to select a switching state acting towards a reduction of the asymmetry if a voltage space vector being non-unique with respect to the converter switching state occurs. This switching state has to be included into the switching sequence while a minimum number of switchings has to be considered (cf. [4], p. 21). For the time-average over a mains period this leads to an increase of the relative on-time of the switching states which effect a reduction of the unsymmetrical voltage distribution. The relative on-times of the redundant switching states (which would increase the asymmetry) are

reduced by the same amount. For ideal symmetry of the output partial voltages the redundant switching-states have equal on-times. Respective modulation methods are given in literature especially for three-level PWM inverters [5], [6], [7] (e.g., drive inverters for high power three-phase AC locomotives [8]). The coordination of the switching of the inverter bridge legs (based on, e.g., a space vector control unit being included into the current control [6], [9] or flux and torque control [10]) is common to the methods being also applicable for three-level

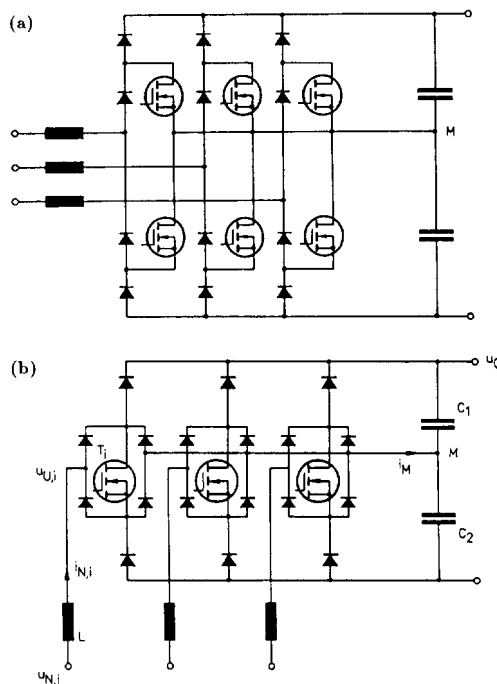


Fig.1: Realization forms of three-phase unidirectional boost-type three-level PWM rectifier systems according to [1] (cf. (a)) and [11] (cf. (b)). The transistors of each bridge leg of the system (a) contained in the positive and negative bridge halves are controlled in phase. For equal pulsing of the corresponding bridge legs (a) and (b) show identical operational behavior regarding generation of the rectifier input voltage and of the center point current.

PWM rectifier systems. However, concerning an application for lower power (5 kW...15 kW, e.g. in the area of telecommunications power supplies [11]) these control methods show the disadvantage (1) of a relative high complexity of the control unit (requiring a digital realization) and (2) of restricted dynamics due to the application of a PWM unit as compared to direct current control [12]. Therefore, for minimizing the system cost we have to pose the question for a possible inclusion of the potential control into a simple analog current control concept. There, the switching decisions shall be derived directly from the control error of the phase currents without considering the resulting overall switching state of the converter (or, without coordination of the switching of the bridge legs).

In this paper a method for control of the output voltage center point of the unidirectional three-level PWM rectifier systems shown in Fig.1 (which has been only briefly discussed in [11]) is analyzed in more detail. This method can be realized easily as practical circuit. The modelling and dimensioning of the center point voltage control circuit are treated. Independent hysteresis controllers are used for a mains voltage proportional guidance of the phase currents. Based on the analysis of the generation of the center point current in dependency on the converter switching state (cf. section 2) in section 3 the stability of the voltage center point is investigated. Also, the transfer function describing the dynamic system behavior is determined. It is shown that an unsymmetry of the output partial voltages without control interaction results in a mean value of the center point current increasing the unsymmetry. Therefore, a stable converter operation is only possible with a control of the center point voltage. As described in section 4, the control of the potential of the output voltage center point can be achieved by an offset (being equal for all phases) of the phase current reference values. Due to the floating mains neutral point the mains current shape is not influenced directly thereby. However, the offset signal influences the distribution of the frequency of the switching states used for guidance of the mains current and therefore of the value of the center point current. Based on the results of a digital simulation in section 5 the design of the center point voltage control circuit of a rectifier unit (being proposed as input circuit of a 8 kW uninterruptible power supply) is described. Finally, in section 6 the controller function for stationary operation and for a loading step of the output voltage center point (e.g., by a converter connected in series) is analyzed.

2 Basic Considerations

For the sake of completeness of this paper we want to discuss briefly the hysteresis control of the mains phase currents (as shown in detail in [11]) and the thereby resulting loading of the output voltage center point.

2.1 Hysteresis Control of the Mains Phase Currents

The current consumption of a boost-type PWM rectifier system is impressed according to

$$L \frac{di_N}{dt} = \underline{u}_N - \underline{u}_U \quad (1)$$

by the difference of the rectifier input voltage space vector \underline{u}_U and the mains voltage space vector

$$\underline{u}_N = \hat{U}_N \exp j\varphi_N \quad \varphi_N = \omega_N t \quad (2)$$

as apparent across the inductances L connected in series on the mains side. For the definition of the complex space vector we have there

$$\underline{u}_U = \frac{2}{3}(u_{U,R} + \underline{a}u_{U,S} + \underline{a}^2u_{U,T}) \quad \underline{a} = \exp j\frac{2\pi}{3} \quad (3)$$

as shown for the example of the rectifier input voltage. A sinusoidal shape of the mains current (corresponding to the mains voltage shape) and resistive mains behavior of the rectifier system

$$\underline{i}_N^* = \hat{I}_N^* \frac{\underline{u}_N}{\hat{U}_N} \quad (4)$$

is obtained ideally for

$$\underline{u}_U^* = \underline{u}_N - j\omega_N L \underline{i}_N^* \quad (5)$$

Due to the discontinuous control property of the converter the fundamental voltage space vector $\underline{u}_{U,(1)} = \underline{u}_U^*$ is generated only as time average over several switchings of the system bridge legs. For the current control error and/or the current harmonics occurring there

$$\Delta \underline{i}_N = \underline{i}_N - \underline{i}_N^* \quad (6)$$

there follows with Eq.(1)

$$L \frac{d\Delta \underline{i}_N}{dt} = \underline{u}_U^* - \underline{u}_U \quad (7)$$

the variation of the control error is defined directly by the difference between the actually generated voltage and the time-continuous varying reference value.

For control of the phase currents by independent hysteresis controllers the control of the bridge legs is derived directly from the control errors of the related phase currents:

$$s_i = \begin{cases} 0 & \text{if } i_{N,i} > i_{N,i}^* + h \\ 1 & \text{if } i_{N,i} < i_{N,i}^* - h \end{cases} \quad (8)$$

There one has to note that forming of a phase voltage $u_{U,i}$ (and, therefore, of the voltage space vector \underline{u}_U) is influenced not only by the switching state of the power transistor T_i (characterized by a binary switching function s_i , $i = R, S, T$) but also by the sign of the corresponding mains current $i_{N,i}$

$$u_{U,i} = \begin{cases} \text{sign}\{i_{N,i}\} \frac{U_\Omega}{2} & \text{if } s_i = 0 \\ 0 & \text{if } s_i = 1 \end{cases} \quad (9)$$

(As the reference point of the voltages $u_{U,i}$ we select the ideal center point of the output voltage). The current dependency of the phase voltages has to be considered by an inversion

$$s_i = \begin{cases} s_i' & \text{if } i_{N,i}^* \geq 0 \\ \text{NOT } s_i' & \text{if } i_{N,i}^* < 0 \end{cases} \quad (10)$$

controlled by the sign of the corresponding mains current reference value (cf. Fig.3).

Basically, each phase has three possible phase voltage values, $+\frac{U_\Omega}{2}$, 0 and $-\frac{U_\Omega}{2}$ (three-phase *three-level* PWM rectifier). In total, there result $3^3 = 27$ possible states of the converter system. However, due to the dependency of the voltage generation on the sign of the mains phase currents (cf. Eq.(9)) in each phase there is always only one switching between two voltage levels ($+\frac{U_\Omega}{2}$ and 0 for $i_{N,i} > 0$; $-\frac{U_\Omega}{2}$ and 0 for $i_{N,i} < 0$) possible. Therefore, there remain $2^3 = 8$ phase voltage combinations for each combination of current flow directions (e.g., $i_{N,R} > 0$, $i_{N,S} < 0$, $i_{N,T} < 0$).

Because the rectifier system has no connection between the DC side (e.g. of the output voltage center point) and the mains star point, the formation of the mains phase currents is not defined by the phase voltages but by the line-to-line voltages and/or by the voltage space vectors \underline{u}_U corresponding to the eight phase voltage combinations ($u_{U,R}, u_{U,S}, u_{U,T}$) and/or switching state combinations. There, only 7 voltage space vectors (cf. Fig.2) are related to the eight phase voltage combinations (and/or switching state combinations). There exists a redundancy of switching states (equal to a degree of freedom of the voltage control) regarding the formation of the voltage space

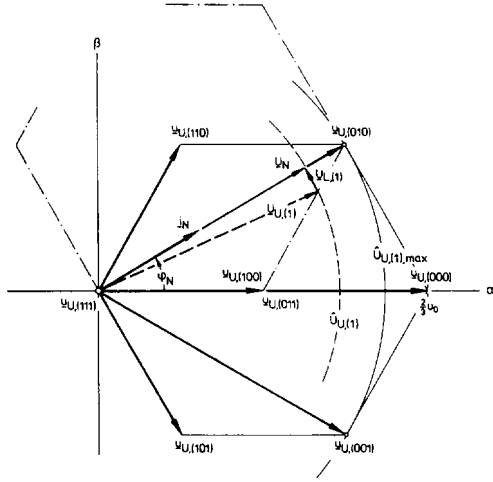


Fig.2: Voltage space vectors of a unidirectional three-phase three-level PWM rectifier system for $i_{N,R} > 0, i_{N,S} < 0, i_{N,T} < 0$ and/or $\varphi_N \in (-\frac{\pi}{6}, +\frac{\pi}{6})$. The momentary switching state of the bridge legs is marked by the triple of values (s_R, s_S, s_T) formed by the phase switching functions. Furthermore shown are: trajectory of the space vector of the rectifier input voltage fundamental $\underline{u}_{U,(1)} = \underline{u}_U^*$ (defined by Eq.(5)); $\underline{u}_{L,(1)}$: space vector of the fundamental voltage drop across the series inductances L .

vectors. As shown in section 4, this degree of freedom can be applied for controlling the center point potential.

Based on a purely sinusoidal (if the ripple with switching frequency is neglected) symmetrical mains phase current shape

$$\begin{aligned} i_{N,R} &= \hat{I}_N \cos(\varphi_N) \\ i_{N,S} &= \hat{I}_N \cos(\varphi_N - \frac{2\pi}{3}) \\ i_{N,T} &= \hat{I}_N \cos(\varphi_N + \frac{2\pi}{3}), \end{aligned} \quad (11)$$

there results always at the limits of $\frac{\pi}{3}$ wide intervals $\varphi_N \in (-\frac{\pi}{2}, -\frac{\pi}{6}), (-\frac{\pi}{6}, +\frac{\pi}{6}), (+\frac{\pi}{6}, \frac{\pi}{2})$, etc. a reversal of the sign of a phase current (e.g., of the current $i_{N,T}$ in $\varphi_N = -\frac{\pi}{6}$ or of the phase current $i_{N,S}$ in $\varphi_N = +\frac{\pi}{6}$). By the inversion of the corresponding phase voltage connected herewith the hexagon formed by the rectifier input voltage space vectors (cf. Fig.2) is being rotated by $\frac{\pi}{3}$ in the direction of the

the movement of the current space vector. Therefore, the vectors being available for formation of \underline{u}_U^* lie always symmetrical about the angular segment corresponding to the momentarily valid combination of the sign and/or directions of the phase currents.

The block diagram of the control of the rectifier system is shown in Fig.3. According to Eq.(4) the mains phase current reference values are given proportional to the corresponding mains phase voltages. The amplitudes of the phase currents are defined by an output voltage control loop $F(s)$ in dependency on the control error of the output voltage $\Delta u_O = u_O^* - u_O$.

2.2 Loading of the Output Voltage Center Point for Hysteresis Control of the Phase Currents

As already mentioned in section 1, the control unit of the converter has to guarantee (besides guidance of the mains phase currents and controlling the output voltage) also the symmetry

$$u_{C,1} = u_{C,2} = \frac{U_O}{2} \quad (12)$$

of the partial output voltages. Only by this one can avoid unequal voltage and current stress on the components of the positive and negative bridge halves. There, the basis of controlling the potential of the center point M is given by the knowledge of the center point currents i_M resulting for different switching states (s_R, s_S, s_T) . Therefore, in the following we will investigate in more detail the average shift of the center point potential occurring within the $(\frac{\pi}{3})$ wide intervals of the mains period which have to be considered separately with regard to the voltage formation.

An unsymmetry of the capacitor voltages $u_{C,1}$ and $u_{C,2}$ there is characterized by the center point voltage

$$u_M = \frac{1}{2}(u_{C,2} - u_{C,1}) \quad (13)$$

related to the ideal output voltage center point. Considering $u_{C,1} + u_{C,2} = U_O$ we have there

$$u_{C,2} = \frac{1}{2}U_O + u_M \quad u_{C,1} = \frac{1}{2}U_O - u_M. \quad (14)$$

The current i_M being a load for the capacitive center point is formed in dependency on the switching states of the power transistors T_i by sections of the phase currents

$$i_M = s_R i_{N,R} + s_S i_{N,S} + s_T i_{N,T}. \quad (15)$$

For the voltage shift of the center point there follows

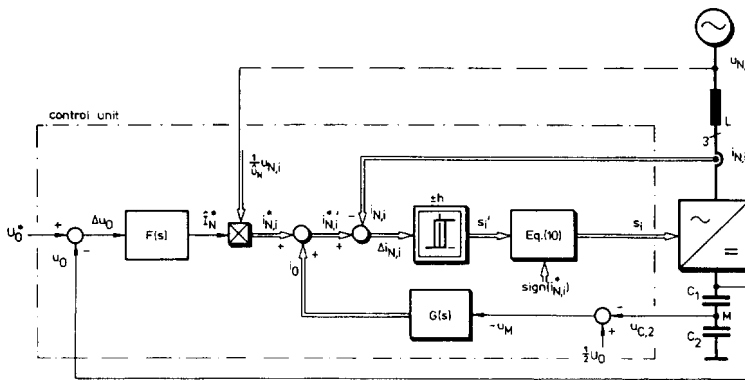


Fig.3: Block diagram of the control of a three-phase three-level PWM boost rectifier. $F(s)$: control of the output voltage u_O ; $G(s)$: control of the potential of the capacitive output voltage center point M (cf. section 5.2); inner control loop: hysteresis control of the phase currents $i_{N,i}, i = R, S, T$; the switching decisions of the hysteresis switching elements are inverted according to Eq.(10) for $i_{N,i}^* < 0$. For the sake of clarity signal paths equivalent for all phases are combined into double lines for all phases.

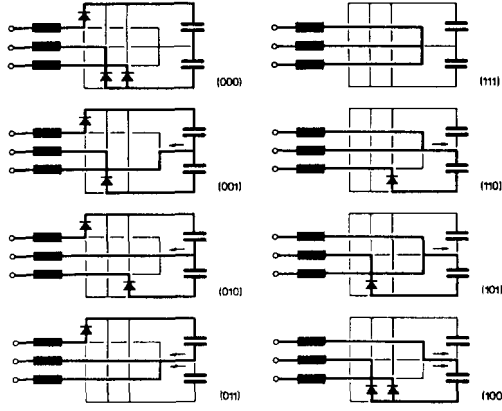


Fig.4: Basis for determination of the center point current i_M in dependency on the converter switching state (marked by (s_R, s_S, s_T)) for $\varphi_N \in (-\frac{\pi}{6}, +\frac{\pi}{6})$ and/or $i_{N,R} > 0, i_{N,S} < 0$ and $i_{N,T} < 0$.

$$\frac{du_M}{dt} = \frac{1}{2C} i_M \quad (16)$$

for constant output voltage $u_O = U_O$ and/or $\frac{du_{C,1}}{dt} = -\frac{du_{C,2}}{dt}$ with Eq.(13) and $C_1 = C_2 = C$. Due to an influence of $u_{C,1}$ and $u_{C,2}$ in the same direction by the load-side current flow the variation of the center point voltage is determined only by i_M . Due to the constant output voltage (being guaranteed by the output voltage controller $F(s)$) the parallel connection $2C$ of both capacitors is acting.

The center point currents (cf. Eq.(15)) resulting for the possible combinations of values of the phase switching functions for $\varphi_N \in (-\frac{\pi}{6}, +\frac{\pi}{6})$ (and/or $i_{N,R} > 0, i_{N,S} < 0, i_{N,T} < 0$ and $i_{N,R} > |i_{N,S}|, |i_{N,T}|$) can be taken directly from Fig.4. Also, they are summarized in Tab.1. For equal frequency (equal relative on-time and equal distribution within the angle interval φ_N) there results no mean potential shift of the capacitor center point as a sum of the contributions $(\frac{du_M}{dt})_{avg}$ of the different switching states. However, for hysteresis control of the phase currents the switching states resulting in a lower current variation $\frac{d\Delta i_M}{dt}$ (in other words: the space vectors $\underline{u}_{U,(010)}, \underline{u}_{U,(100)}, \underline{u}_{U,(011)}, \underline{u}_{U,(001)}, \underline{u}_{U,(000)}$ lying in the vicinity of the trajectory of the ideally to be formed space vector \underline{u}_U^*) have a greater mean existence interval and/or higher relative on-time δ . Therefore, as shown in Tab.1, for the considered segment of the mains period there results a negative mean value $i_{M,avg}$ and/or an increase of $u_{C,1}$ relative to $u_{C,2}$ ($i_{M,avg}$ denotes averaging over a $\frac{\pi}{3}$ wide interval).

An analog analysis of the center point current for the angle interval $\varphi_N \in (+\frac{\pi}{6}, +\frac{\pi}{2})$ and/or $i_{N,R} > 0, i_{N,S} > 0$ and $i_{N,T} < 0$ (cf. Fig.5) leads to the results compiled in Tab.2. There results (contrary to the previous considerations) a positive mean value $i_{M,avg}$.

The analysis of further angle intervals leads to alternating positive and negative contributions $i_{M,avg}$. As known also from three-level PWM inverter circuits [13], the fundamental frequency of the center point current i_M is defined by $3f_N$, therefore.

Based on the previous considerations and on ideally equal system behavior within the different angle intervals one would not expect a potential shift in the average over a mains period. However, there results (due to the mutual influence of the current controllers, being characteristic for three-line systems and independent current controllers, cf. [14], p. 297 or [16], p. 423) a stochastic (chaotic [15]) sequence and/or very much varying on-times and distributions of the different switching states. As a digital simulation proves, the center point cur-

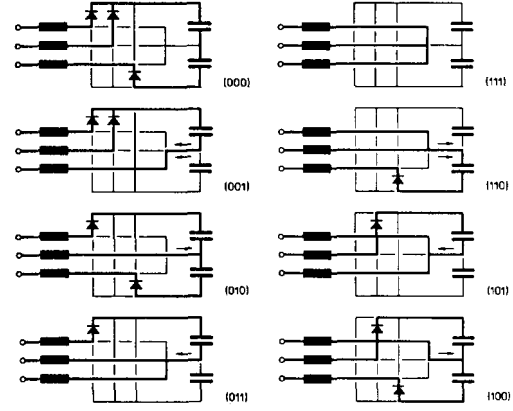


Fig.5: As Fig.4, but $\varphi_N \in (+\frac{\pi}{6}, +\frac{\pi}{2})$ and/or $i_{N,R} > 0, i_{N,S} > 0$ and $i_{N,T} < 0$.

rent i_M shows in general a (small) DC component I_M (mean value over a mains period) or a low frequency harmonic (lying below the mains frequency), therefore. This leads to an unsymmetry of the partial output voltages and/or to a shift U_M (mean value over a mains period) of the output voltage center point.

s_R	s_S	s_T	i_M	$(\frac{du_M}{dt})_{avg}$	$\delta(\frac{du_M}{dt})_{avg}$
0	0	0	0	0	0
0	0	1	i_T	-	--
0	1	0	i_S	-	--
0	1	1	$-i_R$	--	--
1	0	0	$+i_R$	++	++
1	0	1	$-i_S$	+	+
1	1	0	$-i_T$	+	+
1	1	1	0	0	0

Tab.1: Center point current i_M and average shift of the center point potential u_M within the angle interval $\varphi_N \in (-\frac{\pi}{6}, +\frac{\pi}{6})$ due to a converter switching state (s_R, s_S, s_T) for equal relative on-time and distribution of the switching states (cf. $(\frac{du_M}{dt})_{avg}$) and for the relative on-time δ as actually resulting for hysteresis control of the mains phase currents (and for values of the voltage transformation ratio $M = \frac{U_O}{\sqrt{3}U_N}$ close to 1). There results a negative mean value of the center point current and/or an increase of the partial output voltage $u_{C,1}$ relative to $u_{C,2}$.

s_R	s_S	s_T	i_M	$(\frac{du_M}{dt})_{avg}$	$\delta(\frac{du_M}{dt})_{avg}$
0	0	0	0	0	0
0	0	1	i_T	--	--
0	1	0	i_S	+	++
0	1	1	$-i_R$	-	-
1	0	0	$+i_R$	+	++
1	0	1	$-i_S$	-	-
1	1	0	$-i_T$	++	++
1	1	1	0	0	0

Tab.2: As Tab.1 but $\varphi_N \in (+\frac{\pi}{6}, +\frac{\pi}{2})$ and/or $i_{N,R} > 0, i_{N,S} > 0$ and $i_{N,T} < 0$.

A small (mean) unsymmetry of the partial output voltages could be acceptable for appropriate dimensioning of the power semiconductor devices. However, regarding a possible converter operation without control of the center point voltage one has to pose the question whether the occurrence of a potential shift U_M leads to an increase or decrease of the mean current value I_M resulting in the unsymmetry. From a controls point-of-view we therefore have to analyze the inherent stability of the center point. These considerations (finally leading to a dynamic model of the system to be controlled by a center point voltage controller) are the topic of the next section.

3 Investigation of the Inherent Stability of the Output Voltage Center Point

3.1 Center Point Current for Unsymmetrical Partial Voltages

The analysis of the stability is based on a (small) shift U_M of the capacitive center point. The thereby resulting mean value I_M is calculated by digital simulation. For the sake of a clearer representation of the relevant conditions we will use a specific numerical example. It is based on the rated operational parameters

$$\begin{aligned} P_O &= 8 \text{ kW} \\ U_O &= 700 \text{ V} \\ U_N &= 230 \text{ V}_{\text{rms}} \\ \hat{I}_N &= 18 \text{ A} \\ h &= 1.5 \text{ A} \end{aligned} \quad (17)$$

as given for the application of a three-phase three-level PWM boost rectifier for the power supply of the DC link of an UPS where low effects on the mains are required. (There, the efficiency of the entire unit is estimated as $\eta \approx 0.91$.) Furthermore, with regard to an average switching frequency $f_P \approx 38 \text{ kHz}$ we choose

$$L = 0.3 \text{ mH} , \quad (18)$$

and for the capacitance of the output capacitors C_1 and C_2

$$C = 2000 \text{ } \mu\text{F} . \quad (19)$$

As Fig. 6 shows, for a deviation of the partition of the output voltage from the ideal symmetry, there results a mean value I_M acting in the direction of increased unsymmetry and being proportional (in a first approximation) to the unsymmetry U_M .

For a control-oriented modelling this behavior has to be described by a positive feedback

$$g_M = \frac{\Delta I_M}{\Delta U_M} \quad g_M > 0 \quad (20)$$

corresponding to the positive rate of rise of the characteristic $I_M = I_M\{U_M\}$ in $U_M = 0$. Therefore, the system to be controlled by the center point voltage control shows a pole in the right-hand s -half-plane

$$S(s) = \frac{1}{s - \frac{g_M}{2C}} . \quad (21)$$

A clear explanation of the operational behavior of the system can be found via the analysis of the voltage generation of the converter as given for unsymmetry of the output partial voltages. There, according to

$$\underline{u}_U' = \underline{u}_U + \Delta \underline{u}_U \quad (22)$$

a distortion space vector $\Delta \underline{u}_U$ is correlated with each of the converter switching states. Its addition to the vector \underline{u}_U given for $u_M = 0$ leads to the voltage space vector resulting for unsymmetry. There follows (cf. Eq.(3) and Eq.(9))

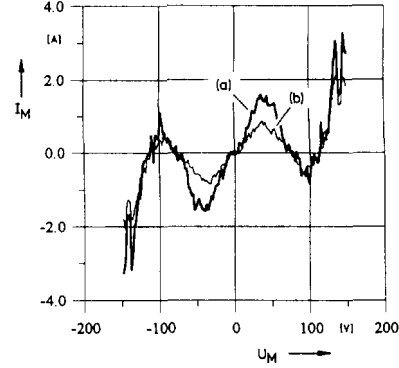


Fig.6: Dependency of the mean value I_M (related to a mains period) of the center point current i_M on the (mean) center point potential shift U_M for $\hat{I}_N^* = 18 \text{ A}$ (cf. (a)) and $\hat{I}_N^* = 9 \text{ A}$ (cf. (b)). The characteristics can be replaced with sufficient accuracy by a straight line $I_M \approx I_{M, U_M=0} + g_M U_M$ in the vicinity of $U_M = 0$. According to Eq.(15) the gain g_M shows an approximately proportional dependency on the amplitude \hat{I}_N^* of the mains phase current reference values; $\hat{I}_N^* = 18 \text{ A}$: $g_M \approx 0.04$, $\hat{I}_N^* = 9 \text{ A}$: $g_M \approx 0.02$.

$$\Delta \underline{u}_U = \frac{2}{3} u_M (s_R + a s_S + a^2 s_T) . \quad (23)$$

The distortion space vectors given within the interval $\varphi_N \in (-\frac{\pi}{6}, +\frac{\pi}{6})$ are shown in Tab.3.

s_R	s_S	s_T	$\Delta \underline{u}_U$
0	0	0	0
0	0	1	$+\frac{2}{3} u_M a^2$
0	1	0	$+\frac{2}{3} u_M a$
0	1	1	$-\frac{2}{3} u_M$
1	0	0	$+\frac{2}{3} u_M$
1	0	1	$-\frac{2}{3} u_M a$
1	1	0	$-\frac{2}{3} u_M a^2$
1	1	1	0

Tab.3: Distortion space vectors (cf. Eq.(22)) in dependency on the converter switching state for $\varphi_N \in (-\frac{\pi}{6}, +\frac{\pi}{6})$.

If the capacitive center point M is not loaded (switching states (000) and (111)) a potential shift U_M does not influence the corresponding voltage space vectors. In this case, the voltage conditions (decoupling of the zero component) at the converter input being relevant for the mains current generation are only determined by the total amount of the output voltage. The distortion space vectors $\Delta \underline{u}_U$ of the remaining switching states show a constant absolute value being defined directly by the unsymmetry. The conditions given for $u_M < 0$ are shown in Fig.7.

As already described in section 2.2, for hysteresis current control the frequency of the switching states is essentially influenced by the absolute values of the corresponding space vectors $\frac{d\Delta \underline{u}_U}{dt}$ defining the time behavior of the control error. E.g., in $\varphi_N \in (-\frac{\pi}{6}, +\frac{\pi}{6})$ the switching states (010), (000), (001) and (100)/(011) (lying in the immediate vicinity of the trajectory of the space vector \underline{u}_U' , cf. Fig.2) are preferred. According to Fig.7, an asymmetry u_M leads especially to a change of the absolute value of the space vectors $\underline{u}_{U,(100)}$ and $\underline{u}_{U,(011)}$ with the same amount in the opposite directions, besides a rotation of the vectors of the switching states (010) and (001). Therefore, for $u_M < 0$ the switching state (011) is preferred as compared to (100) (cf. Fig.7 and Fig.8). As can be seen from Tab.1 with this the equilibrium of the

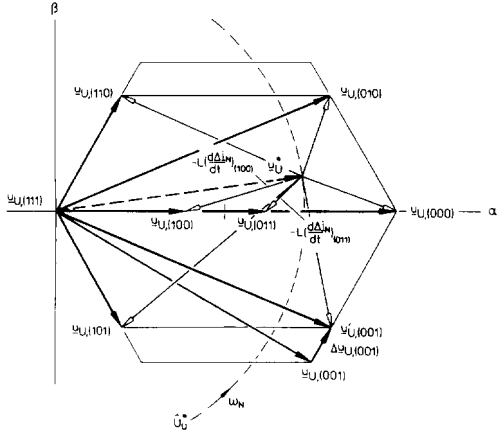


Fig. 7: Voltage space vectors of a unidirectional three-phase three-level PWM rectifier system for $\varphi_N \in (-\frac{\pi}{6}, +\frac{\pi}{6})$ ($i_{N,R} > 0, i_{N,S} < 0, i_{N,T} < 0$ for asymmetry $U_M < 0$ ($U_{C,1} > U_{C,2}$) of the partial output voltages. As shown for switching state (001), the space vector \underline{u}_U' resulting for asymmetry can be thought as being generated by shifting $\Delta \underline{u}_U$ of the vector \underline{u}_U given for symmetry $u_M = 0$ (cf. Eq.(22)).

switching states which have essential influence on generating the center point current is disturbed. In consistency with Fig.6 there occurs a reduction of the negative average value $i_{M,avg}$ which further increases the asymmetry.

As a detailed analysis shows, the considerations given so far for $\varphi_N \in (-\frac{\pi}{6}, +\frac{\pi}{6})$ correctly represent the conditions within the entire fundamental period. For each $\frac{\pi}{3}$ -wide interval of the mains period (to be differentiated concerning the sign combinations of the phase currents) there results a change of the respective average value $i_{M,avg}$ which acts in the direction of an increase of an (already) existing asymmetry.

One has to note that (as being immediately clear from Fig.7) the voltage transfer ratio of the converter

$$M = \frac{U_O}{\sqrt{3}U_N} \quad (24)$$

takes essential influence on the value of the gain g_M . A reduction of the mains voltage (increase of M) and/or relative reduction of the peak value $\hat{U}_U \approx \hat{U}_N$ (defining the trajectory of the space vector \underline{u}_U') results in an increase of the gain g_M for $M \in [1, \sqrt{3}]$. This is true because then in general a larger relative on-time of the switching states (001) and (100) is given. Also, for equal asymmetry $u_M < 0$ a larger reduction of the absolute value of the vector $(\frac{d\Delta \underline{u}_U}{dt})_{(011)}$ is given.

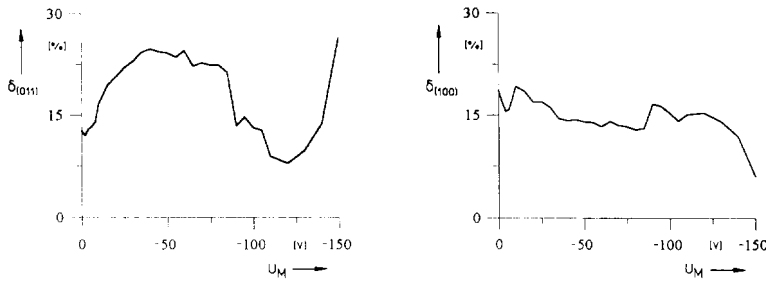


Fig. 8: Analysis (corresponding to Fig.7) of the increase and/or decrease of the relative on-time δ of the switching states (011) and (100) (related to $\frac{\pi}{3}$) in dependency on the shift $U_M < 0$ of M .

Remark: For $M > \sqrt{3}$ ($\hat{U}_U < \frac{1}{3}U_O$) the sign of g_M is reversed, there exists inherent stability of M . In this case one could theoretically omit a control of the output voltage center point potential u_M . Due to the voltage transfer ratios lying typically close to $M = 1$ for boost PWM rectifier systems this case (which would be of importance practically only for the requirement of a wide input voltage range) shall not be discussed here in more detail.

3.2 Center Point Current for Asymmetry of the Mains Phase Voltages

Besides an analysis of the dependency of the average value I_M on an asymmetry U_M of the partial output voltages also the influence of an asymmetry of the mains phase voltages on generating the center point current has to be analyzed. An investigation based on an amplitude error or a phase error of a phase voltage shows a very minor influence of the center point current by the mains voltage conditions, however (cf. Fig.9). Due to the usually minor asymmetry of the mains in practical applications this influence shall be neglected in the following.

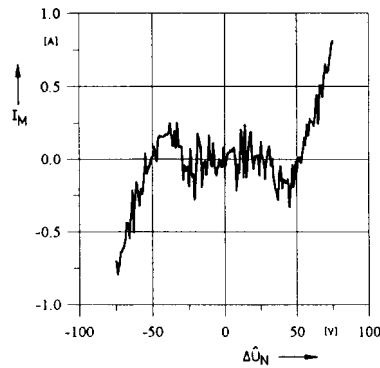


Fig. 9: Details concerning the analysis of the influence of an asymmetry of the mains phase voltages on generating a mean value I_M of i_M ; ΔU_N : amplitude error of a phase voltage.

4 Control Concept

As noted in section 2.1, the three-level PWM rectifier system has two identical (redundant) switching states (e.g., (100) and (011) for $\varphi_N \in (-\frac{\pi}{6}, +\frac{\pi}{6})$, cf. Fig.2) regarding the generation within each $\frac{\pi}{3}$ wide interval of the mains period. (This interval corresponds to a specific combination of the signs of the mains phase currents.) The redundant

switching states of an interval (1) lead to opposite signs of the center point current and (2) have essential influence on the generation of the center point current (cf. e.g., (100) and (001) in Tab.1). Therefore, a shift and/or control of the center point potential can be achieved without influencing of the output voltage control and/or the mains current control. There, we have (in general) to increase the relative on-time of the redundant switching state acting in the direction of a reduction of an existing potential shift (or, to reduce the relative on-time of the inverse (redundant) switching state).

As a more detailed analysis shows, we can generate the redundant switching states (leading to $\frac{du_M}{dt} > 0$) within each sign interval (i.e., within the entire mains period) starting from $(s_R', s_S', s_T') = (111)$. The same is true for $\frac{du_M}{dt} < 0$ for the inverse switching states, starting from the combination of the inverse values $(s_R', s_S', s_T') = (000)$. This becomes clear for generating the actual switching state s_i under consideration of the sign-dependent inversion of the switching decisions s_i' of the hysteresis switching elements in dependency on the sign of the phase currents (cf. Eq.(10)). E.g., we have to invert the phase switching functions s_S' and s_T' for $\varphi_N \in (-\frac{\pi}{6}, +\frac{\pi}{6})$ according to $i_{N,R}^* > 0$, $i_{N,S}^* < 0$ and $i_{N,T}^* < 0$. It confirms the previous statement that we have to correlate the redundant switching state $(s_R, s_S, s_T) = (100)$ (leading to $\frac{du_M}{dt} > 0$) with $(s_R', s_S', s_T') = (111)$ and the redundant switching state $(s_R, s_S, s_T) = (011)$ (leading to $\frac{du_M}{dt} < 0$) with $(s_R', s_S', s_T') = (000)$.

In summary, we have to, therefore, increase the switching frequency f_+ of the positive switching thresholds $i_{N,i}^* + h$ for correcting a potential shift $U_M > 0$ of hysteresis control of the phase currents (and, vice versa, to decrease the switching frequency f_- of the negative switching thresholds $i_{N,i}^* - h$). Accordingly, for $U_M < 0$ a reduction of f_+ as compared to f_- has to be observed. As the following section shows, this can be achieved by an offset signal i_0 of the mains phase current reference.

4.1 Mains Current Hysteresis Control for Offset of the Phase Current Reference Values

Because the control signals s_i' (and, therefore, the converter switching state (s_R, s_S, s_T)) is derived directly from the difference between reference and actual value of each phase current according to the function of the hysteresis control, the possibility of a control input influencing the frequency of the different switching states is limited basically to a modification of the reference value shape. Due to the amplitude \hat{I}_N being fixed by the power to be supplied and by the required sinusoidal shape, here the only degree of freedom consists of the addition of a zero-component i_0

$$\begin{aligned} i_{N,R}^* &= i_{N,R}^* + i_0 \\ i_{N,S}^* &= i_{N,S}^* + i_0 \\ i_{N,T}^* &= i_{N,T}^* + i_0 \end{aligned}$$

(i.e., of an offset being equal for all phases).

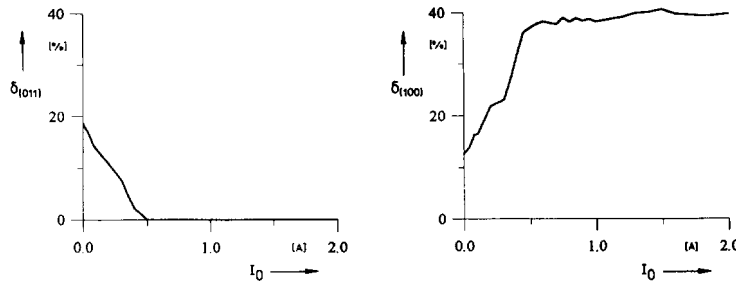


Fig.11: Average relative on-times $\delta_{(100)}$ and $\delta_{(011)}$ of the redundant switching states (100) and (011) being given for $\varphi \in (-\frac{\pi}{6}, +\frac{\pi}{6})$, for hysteresis control of the phase currents and offset $i_0 = I_0$ of the phase current reference values.

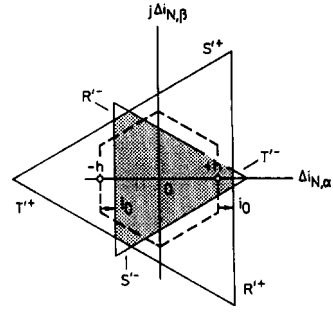


Fig.10: Tolerance area of a hysteresis current control for space vector representation $\Delta \underline{i}_N$ of the phase current control errors $\Delta i_i = i_i - i_i^*$ ($i = R, S, T$) and offset $I_0 > 0$ of the phase current reference values. R'^+, S'^+, T'^+ : positive switching thresholds; there occurs a state change $s_i' = 1 \rightarrow 0$ for switching over; R'^-, S'^-, T'^- : negative switching thresholds, for switching over a state change $s_i' = 0 \rightarrow 1$ occurs; tolerance area for $I_0 = 0$ shown hatched.

Because the rectifier system has no connection to the mains neutral point, the sum of the mains phase currents is being forced to 0 at all times

$$i_{N,R} + i_{N,S} + i_{N,T} \equiv 0. \quad (25)$$

Therefore, the offset i_0 cannot be set by the phase current controllers and does not lead to a direct influence on the mains current shape.

As an analysis of the system behavior, related to a space vector representation

$$\begin{aligned} \Delta i_{N,\alpha} &= \Delta i_{N,R} - i_0 \\ \Delta i_{N,\beta} &= \frac{1}{\sqrt{3}}(\Delta i_{N,S} - \Delta i_{N,T}) \end{aligned} \quad (26)$$

of the control errors of the phase currents $\Delta i_i = i_i - i_i^*$ clearly shows, i_0 has influence on the form of the tolerance area (cf. Fig.10) being defined by the intersection of the tolerance bands of the phase current controllers. Therefore, it has influence on the frequency of the switching states (and/or the value of the center point current) being used for guidance of the mains current.

For $i_0 = 0$ the tolerance area shows the characteristic form of an equilateral hexagon (cf. Fig.14 in [16]). It is limited by segments of the positive and negative switching thresholds of equal length (cf. Fig.10). Accordingly, for both switching thresholds there exists equal switching frequency ($f_+ = f_-$).

If now the switching thresholds (and/or the tolerance bands) are shifted due to an offset i_0 of the phase current reference values

$$s'_i = \begin{cases} 0 & \text{if } i_{N,i} > i_{N,i}^* + h + i_0 \\ 1 & \text{if } i_{N,i} < i_{N,i}^* - h + i_0 \end{cases} \quad (27)$$

the tolerance area is being distorted. Also, the border is formed by segments of the positive and negative switching thresholds of unequal length.

For $I_0 > 0$ according to Fig.10 an increase of the contribution of the negative switching thresholds is given there. Accordingly, for (predominant) guidance of Δi_N within the tolerance area the switching frequency f_- is increased (and f_+ decreased accordingly). Therefore, switching states $(s_R', s_S', s_T') = (1xx), (x1x), (xx1)$ are taken on with priority over switching states $(s_R', s_S', s_T') = (0xx), (x0x), (xx0)$. In the average over the mains period there results a tendency in the direction of a the value combination $(s_R', s_S', s_T') = (111)$ (related to $\frac{dU_M}{dt} > 0$ as stated previously). The relative on-time of the value combination $(s_R', s_S', s_T') = (000)$ related to $\frac{dU_M}{dt} < 0$ is reduced accordingly. These considerations are verified clearly, e.g., by the analysis (shown in Fig.11) of the average relative on-times $\delta_{(100)}$ and $\delta_{(011)}$ of the redundant switching states (100) and (011) given for $\varphi \in (-\frac{\pi}{6}, +\frac{\pi}{6})$.

For $I_0 < 0$ an analog consideration leads to $f_+ > f_-$ and, therefore, finally to $\frac{dU_M}{dt} < 0$. Therefore, the offset signal I_0 offers the possibility of an active symmetrization of the partial output voltages and/or of a control of the potential of the output voltage center point.

We have to point out that the method described here shows an analogy to a control concept for controlling of u_M proposed in [4] and [13] in connection with controlling three-level inverters by pulse width modulation. In [13], it is shown very clearly how the direct influence on the average value of the center point current by a zero-component u_0 of the phase modulation functions is possible for PWM. This zero-component corresponds to the offset i_0 of the phase current reference values in the case at hand. Due to the attempt of the phase current controllers to impress i_0 despite the missing neutral line, as a result a mean value of the zero-voltage lying between the mains star point and the center point M . This shows that both concepts are mutually corresponding.

Remark: A shift of the phase current reference values by an offset signal is known also from the current control in *two-level PWM inverters* [17]. The offset signal used there contains three times the mains frequency, however. By a distortion of the tolerance area (similar to the method at hand) especially for small output voltages the occurrence of limit cycles (closed symmetric trajectories of the control error space vector) and/or the occurrence of high switching frequencies is avoided. In the case at hand the switching frequency is not essentially influenced by $i_0 = I_0$.

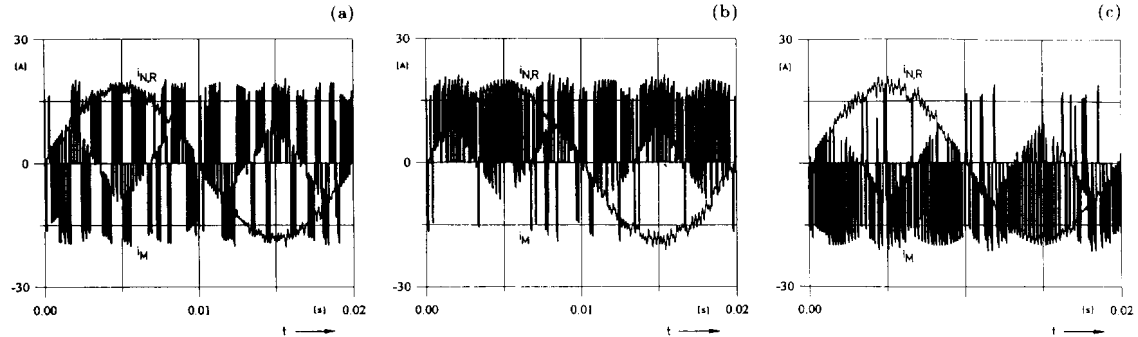


Fig.13: Digital simulation of the time behavior of a mains phase current $i_{N,R}$ and of the center point current i_M for different values I_0 ; representation of a mains period. (a): $I_0 = 0$ (no influence of the current control), $I_M = I_{M,U_M=0} = 0.16$ A; (b): $I_0 = +0.375$ A ($+\frac{1}{4}h$), $I_M = 6.1$ A; (c): $I_0 = -0.375$ A ($-\frac{1}{4}h$), $I_M = -6.0$ A. Operating parameters cf. section 3.1.

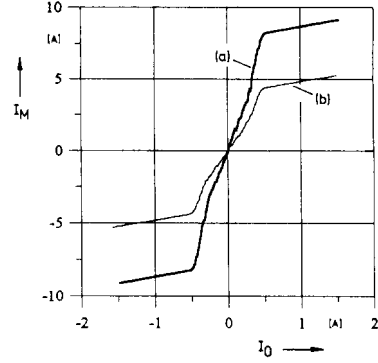


Fig.12: Control characteristic $I_M = I_M \{I_0\}$ of a three-phase unidirectional three-level PWM rectifier for $I_N^* = 18$ A (cf. (a)) and $I_N^* = 9$ A (cf. (b)); the other operating parameters are given in section 3.1.

4.2 Center Point Current for Offset of the Phase Current Reference Values

After the previous considerations we want to calculate the average value I_M resulting for a defined shift I_0 of the reference values and/or the gain

$$k_M = \frac{\Delta I_M}{\Delta I_0} \quad (28)$$

of the output signal I_0 of the center point voltage controller (related to the specific numerical values given in section 3.1) by digital simulation. There, ideal symmetry of the partial voltages, according to $U_M = 0$, and (similar to the calculation of the function $I_M = I_M \{U_M\}$, cf. section 3.1) constant output voltage U_0 and constant amplitude of the phase current reference values I_N^* are assumed. The resulting control characteristic $I_M = I_M \{I_0\}$ is shown in Fig.12. The characteristic can be approximated by a straight line $I_M = I_{M,U_M=0} + k_M I_0$ in the vicinity of the origin. There, $I_{M,U_M=0}$ describes the average value (related to a mains period) of the center point current occurring without control input ($I_0 = 0$) and for symmetric partition $U_M = 0$ of the output partial voltages. For $I_N^* = 18$ A there follows: $I_{M,U_M=0} = 0.16$ A and $k_M = 16$.

As becomes immediately clear by consideration of Eq.(15) and as is

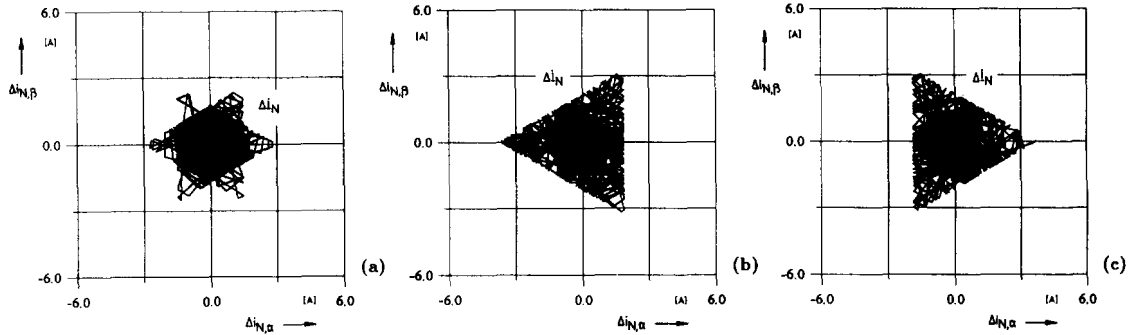


Fig.14: Trajectories of the space vector Δi_N of the phase current control errors corresponding to Fig.13. (a): $I_0 = 0$; (b): $I_0 = +0.375$ A; (c): $I_0 = -0.375$ A.

verified by Fig.12, the center point current I_M shows (in a first approximation) a linear dependency on the amplitude \hat{I}_N^* of the phase current reference values.

Concerning the dependency on the voltage transfer ratio M we have to note that (similar to the considerations described in section 3.1 for g_M) a reduction of the mains voltage amplitude \hat{U}_N and/or an increase of the transfer ratio M leads to an increase of the absolute value of I_M resulting for a defined value I_0 .

The characteristic bend in the control characteristic for $I_0 = \pm \frac{1}{3} \hat{I}_N$ becomes clear by inspection of Fig.10. E.g., for $I_0 = +\frac{1}{3} \hat{I}_N$ the positive switching thresholds are touched by the tolerance area always only in one point now. Therefore, the tolerance area takes on the form of a triangle and is limited exclusively by negative switching thresholds. As becomes immediately clear, thereby the limit of an approximately linear (moving in opposite directions) influence on the relative on-times δ_+ and δ_- of the redundant switching states by I_0 is reached. For a further increase of I_0 (being of no importance in practice) there results further only a small increase of the average value I_M .

For illustrating the conditions, in Fig.13 there is shown always the shape of a mains phase current (phase R) and of the center point current i_M corresponding to a discrete value I_0 . The trajectories of the space vector Δi_N (cf. Eq.(26)) resulting there are summarized in Fig.14.

In connection with the shift I_0 of the phase current reference values there is, finally, to pose the question concerning the occurrence of low frequency harmonics, especially such of even order (due to the unsymmetry, caused by I_0 , of the positive and negative half cycles).

As an analysis of the amplitude spectrum of the periodically continued current shape of a mains period shows (cf. Fig.15), the low frequency spectral components of the mains current are significantly influenced only for very large values I_0 . For the stationary value $I_0, U_M=0 = \frac{1}{k_M} I_M, U_M=0$ being adjusted in practice by the center point voltage controller there results no low frequency distortion of the mains currents (in the case at hand there follows $\hat{I}_N^* = 18$ A $I_0, U_M=0 = 0.01$ A).

5 Controller Design

5.1 Block Diagram of the Control

The block diagram for the control of the center point voltage resulting from a compilation of the considerations of the previous sections is shown in Fig.16. It shall be applied in the following for dimensioning the center point voltage controller $G(s)$.

Basically, the center point voltage control represents a fixed command control $U_M^* = 0$. Therefore, the control loop has to be designed with respect to its disturbance response. A disturbance of the symmetrical voltage partition can result, e.g., from a change of the system load status. There, the output voltage controller $F(s)$ changes the amplitude of the mains phase current reference values within a mains period. Due to the direct coupling between center point current and mains current (cf. Eq.(15)) this results in the occurrence of a transient mean value of i_M . A direct loading of M can result from an asymmetric partition of the load being supplied by the rectifier among the partial output

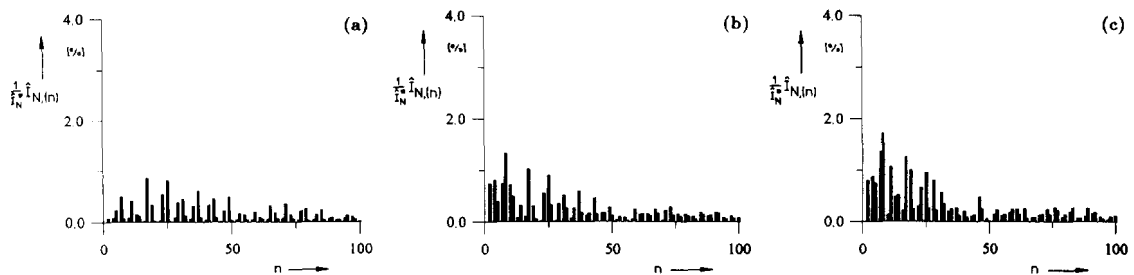


Fig.15: Amplitude spectrum of the mains current (related to the amplitude \hat{I}_N^* of the phase current reference values) of a three-phase hysteresis controlled three-level PWM rectifier system; fundamental not shown; n : number of harmonic; representation for (a): $I_0 = 0$, (b): $I_0 = 0.2$ A and (c): $I_0 = 0.4$ A; operating parameters cf. section 3.1.

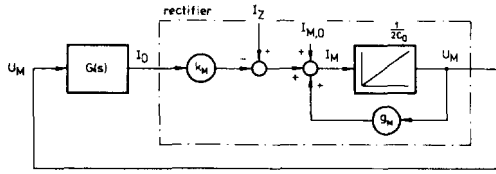


Fig.16: Block diagram of the center point voltage control based on averaging of the quantities U_M and I_M related to a mains period. $G(s)$: center point voltage controller; g_M : influence of an (average) asymmetry U_M of the partial output voltages on I_M ; k_M : gain of the control input I_0 (offset of the mains phase current reference values); $I_{M,U_M=0} = I_{M,0}$: mean value of I_M occurring for ideal symmetry of the output partial voltages; I_Z : disturbance influence.

voltages. Similar conditions are present for supply of a three-phase PWM inverter without special control of the current being taken from the center point. The disturbance influence is considered in Fig.16 by a disturbance current I_Z .

5.2 Design of the Center Point Voltage Controller

As described in section 2.2, the fundamental frequency of the center point current is given by $3f_N$ due to the operating principle of the system. In order to avoid a mutual influence of the phase current control and of the center point voltage control we have to position the cross-over frequency sufficiently far below $3f_N$. Therefore, the model being based on averaging over a fundamental period (cf. Fig.16) can be directly applied for dimensioning of the controller.

If $G(s)$ is realized with respect to stationary accuracy $U_M = U_M^* = 0$ as PI-controller

$$G(s) = k_P + \frac{k_I}{s}, \quad (29)$$

there follows for the disturbance response

$$F_Z(s) = \frac{U_M(s)}{I_Z(s)} = k \frac{s}{1 + 2d \frac{s}{\omega_0} + (\frac{s}{\omega_0})^2} \quad (30)$$

with

$$k = \frac{1}{k_I k_M} \quad \omega_0 = \sqrt{\frac{k_I k_M}{2C}} \quad d = \frac{k_P k_M - g_M}{2\sqrt{2C} k_I k_M}. \quad (31)$$

Therefore, for a step function disturbance $I_Z(s) = \frac{I_Z}{s}$ the center point potential shows a shape corresponding to an impulse response of a PT_2 transfer function with gain k , characteristic frequency ω_0 and damping d . Based on the rated representation of the impulse response of a PT_2 transfer function (cf. e.g., [18], p. 123) we can directly calculate the controller parameters k_P and k_I (cf. Eq.(31)) to be used for a desired transient response and/or damping and characteristic frequency.

For determining the gain k_P of the P-component of the controller we have to consider the limitation of the correcting value being introduced for values $I_0 > \frac{I_N}{3}$ (cf. Fig.12) and the increase of the variation of u_M (frequency $3f_N$, being due to the operating principle) for increasing k_P . In the case at hand $k_P = 0.05$ and $k_I = 1.0$ are assumed. For rated converter load we have $d = 1.5$ and $\omega_0 = 63 \text{ s}^{-1}$, therefore.

For low load there results (due to a decrease of the gains k_M and g_M , which are proportional to the mains current amplitude in a first approximation) a damping reduction of the control loop and a decrease of the characteristic frequency ω_0 (cf. Eq.(31)). As a check for, e.g., $I_N^* = 1.8 \text{ A}$ and/or 10% of the rated power shows (leading to $d = 0.5$, $\omega_0 = 20 \text{ s}^{-1}$) the control shows for the controller parameters given here a sufficient damping behavior and a relatively low settling time, even for low input power.

6 Control Behavior

Finally, we want to verify the function of the center point voltage control by a digital simulation of the converter system. For this purpose, the control behavior is investigated for stationary operation and for a step load of M (e.g., by a converter connected in series to the rectifier system). There, constant output voltage and constant amplitude of the mains current reference values are assumed.

Concerning the assumption of a constant output voltage we have to note, that between control of the partition of the output voltage and the control of the sum of the partial output voltages there is always given a certain dynamic decoupling due to the different dynamics of the respective system to be controlled. For the center point voltage control the dynamically active capacitance of the output circuit is defined by the parallel circuit of the partial capacitors ($2C$), for the output voltage control by the series connection ($\frac{1}{2}C$). Furthermore, the center point current oscillates with three times the mains frequency. This requires a relatively low cross-over frequency of the center point voltage controller (cf. section 5.2). Contrary to this we have ideally constant power flow for output voltage control. Therefore, the controller dimensioning can be performed without taking consideration of a low-frequency variation of the controlled quantity [19].

6.1 Stationary Operation

Figure 17 shows the shape of u_M for closed and open center point voltage control loop. The center point voltage is guided along $u_M^* = 0$ (the reference value) until the control loop is opened in t_1 . As can be expected due to the I-component of the controller $G(s)$ (cf. Eq.(29)), no stationary error results.

If the control input is interrupted ($i_0 = 0$ for $t \in [t_1, t_2]$), the center point potential shows (according to the considerations of section 3.1) a shape corresponding to the step response of an integrator with positive feedback. The step disturbance is given there by the omission of the controller output $k_M I_{0,U_M=0}$ compensating the average value of the center point current $I_{M,U_M=0} = 0.16 \text{ A}$ (cf. Fig.13(a)) resulting due to the statistic sequence of the switching states of the system.

An almost identical shape of the step response of the linear model (cf. Eq.(21)) of the real system is given only in the vicinity of $U_M = 0$ ($|U_M| < 30 \text{ V}$). According to Fig.6, an increasing rise of the asymmetry is connected with a reduction of the positive feedback and, finally, with a sign inversion of g_M . In the case at hand the rate of rise of g_M has negative values in the region $|U_M| = 50 \text{ V} \dots 100 \text{ V}$. Accordingly there is inherent system stability in this operating region. This can

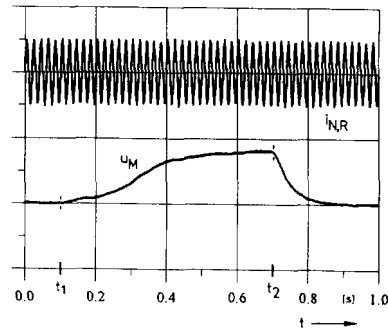


Fig.17: Shape of u_M (100 V/Div) and $i_{N,R}$ (40 A/Div) for open ($t \in [t_1, t_2]$) and closed center point voltage control loop; operating parameters: cf. section 3.1 ($I_N^* = 1.8 \text{ A}$).

be seen in Fig.17 by the motion of the center point voltage towards the zero crossing of the characteristic $I_M = I_M(U_M)$ defining a value $U_M = 80$ V: Due to the high asymmetry of the partial output voltages this operating point is of no importance in practice, however.

Because one strives for a limitation of a (dynamic) asymmetry of the partial output voltages by the control application to typically $\pm 2\% U_O$ (cf. [8], p. 482), one can dimension the controller without considering the change of the system behavior for high asymmetry, however. In the case at hand there is a sufficient accuracy of modelling given up to $\pm 5\% U_O$.

The control loop is closed again in t_2 . Due to the overcritical damping $d = 1.5$ (due to the dimensioning) of the control loop the center point potential shows an aperiodic shape; the asymmetry of the partial voltages is being controlled without overshoot.

Remark: As shown in Fig.17, the sinusoidal guidance of the phase currents is hardly influenced by the asymmetric partition of the output voltage, This is due to the hysteresis control. Also, a relatively large shift of the center point ($U_M \approx 0.1 U_O$) leads to no significant distortion of the mains current shape.

6.2 Dynamic Behavior

For analyzing the dynamic behavior of the center point voltage control the center point M is loaded by a step function of an external current disturbance I_Z . There, value I_Z of the distortion function is fitted to the respective mains current amplitude, i.e., it is changed proportional to the output power of the system. This corresponds (in a first approximation) to the disturbance to be expected for loading of the center point by a converter connected in series.

The shape of the center point potential for $I_Z = 6$ A ($\hat{I}_N = 18$ A) and $I_Z = 0.6$ A ($\hat{I}_N = 1.8$ A) (as determined by digital simulation) is shown in Fig.18. Due to the very good consistency of the characteristic values of the dynamics (damping and characteristic frequency) of the signal shapes with the corresponding considerations in section 5.2 the correctness of modelling and controller dimensioning are verified. As already mentioned in connection with dimensioning of the controller, the dynamic quality of the control is influenced by the output power and/or by the mains current amplitude which influences directly the parameters g_M and k_M . With decreasing output power the oscillation tendency of the system is being increased, the settling time rises accordingly. A control quality being constant for a wide load range can be obtained only by adaption (e.g., by varying the controller gains proportional to $\frac{1}{\hat{I}_N}$, cf. Eq.(31)). An alternative is given by elimination of the load dependency of k_M by a current proportional variation of the hysteresis width.

The amount of the control error is limited to values $< 2\% U_O$. The ripple of the center point voltage u_M is caused by the center point current variations with three times the mains frequency (being due to the operating principle of the system, cf. section 2.2). Due to the open loop gain of the control being $\ll 1$ for $3f_N$ the voltage ripple is hardly influenced by the feedback due to $G(s)$.

7 Conclusions

Essential advantages of the control concept for the potential control of the output voltage center point of a unidirectional three-phase three-level PWM rectifier system as discussed in this paper are (1) the very straightforward realizability by practical circuits and (2) the possibility of a direct inclusion into a high-dynamic (analog) hysteresis control of the mains current. Therefore, the method can be applied also for low-power rectifier systems and for switching frequencies > 100 kHz. A disadvantage would be the lower utilization of the converter switching frequency due to the mutual influence of the phase current controllers

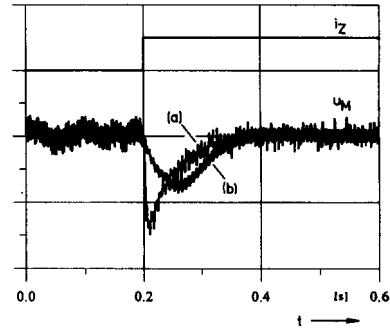


Fig.18: Shape of the center point potential (5 V/div) for load step function of the output voltage center point by a disturbance current $I_Z = \frac{1}{3} \hat{I}_N$; representation for $\hat{I}_N = 18$ A (cf. (a)) and $\hat{I}_N = 1.8$ A (cf. (b)).

as compared to coordinated phase switchings. However, because PWM rectifier systems operate typically with high modulation (M close to 1) one cannot expect an essential reduction of the switching frequency also if optimal (i.e., switching-frequency-minimum and/or predictive, cf. [12], p. 417) hysteresis control is applied (cf. Fig.15(a) in [20]). During further research we want to, therefore, especially experimentally verify the control method. Furthermore, the investigation of the influence of soft-switching techniques (cf. section IV.A in [21] and Figs. 20, 21 in [22]) on the control of the center point is planned, as well as the analysis of the possibility to apply the method in connection with three-level PWM inverter circuits.

References

- [1] Zhao, Y., Li, Y., and Lipo, T. A.: *Force Commutated Three-Level Boost Type Rectifier*. Conference Record of the 28th IEEE Industry Applications Society Annual Meeting, Toronto, Oct. 2-8, Pt. II, pp. 771-777 (1993).
- [2] Kolar, J. W., and Zach, F. C.: *A Novel Three-Phase Three-Switch Three-Level PWM Rectifier*. Proceedings of the 28th Power Conversion Conference, Nürnberg, Germany, June 28-30, pp. 125-138 (1994).
- [3] Tadros, Y., Salama, S., and Höf, R.: *Three-Level IGBT Inverter*. Proceedings of the 23rd IEEE Power Electronics Specialists Conference, Madrid, Spain, June 29 - July 3, Vol. I, pp. 46-52 (1992).
- [4] Steinke, J. K.: *Pulsbreitenmodulationssteuerung eines Dreipunktwechselrichters für Traktionsantriebe im Bereich niedriger Motordrehzahlen*. etzArchiv, Bd. 11, H. 1, pp. 17-24 (1989).
- [5] Klaver, H. L.: *Control of the Neutral Point of a Three-Level Inverter*. Proceedings of the 4th European Conference on Power Electronics and Applications, Firenze, Italy, Sept. 3-6, Vol. 3, pp. 278-281 (1991).
- [6] Bauer, F., and Heining, H. D.: *Quick Response Space Vector Control For a High Power Three-Level Inverter Drive System*. Proceedings of the 3rd European Conference on Power Electronics and Applications, Aachen, Oct. 9-12, Vol. I, pp. 417-421 (1989).
- [7] Liu, H. L., Choi, N. S., and Cho, G. H.: *DSP Based Space Vector PWM for Three-Level Inverter with DC Link Voltage Balancing*. Proceedings of the 17th International Conference on Industrial Electronics, Control and Instrumentation, Kobe, Japan, Oct. 28- Nov. 1, Vol. 1, pp. 197-203 (1991).
- [8] Springmeier, F., and Steinke, J. K.: *Control of the DC Link Neutral Potential of a Three-Level GTO Inverter as a Part of the Direkt Self Control (DSC)*. Proceeding of the 6th Conference on

- Power Electronics and Motion Control, Budapest, Hungary, Oct. 1-3, Vol.2, pp. 479-483 (1990).
- [9] Takeshita, T., and Matsui, N.: *PWM Control and Input Characteristics of Three-Phase Multi-Level AC/DC Converter*. Record of the 23rd IEEE Power Electronics Specialists Conference, Toledo, Spain, June 29 - July 3, Vol. 1, pp. 175-180 (1992).
- [10] Walczyna, A. M., and Hill, R. J.: *Space Vector PWM Strategy for 3-Level Inverters with Direct Self Control*. Proceedings of the 5th European Conference on Power Electronics and Applications, Brighton, UK, Sept. 13-16, Vol. 4, pp. 152-157 (1993).
- [11] Kolar, J. W., and Zach, F. C.: *A Novel Three-Phase Utility Interface Minimizing Line Current Harmonics of High-Power Telecommunications Rectifier Modules*. Record of the 16th IEEE International Telecommunications Energy Conference, Vancouver, Canada, Oct. 30- Nov. 3, pp. 367-374 (1994).
- [12] Holtz, J.: *Pulsewidth Modulation - A Survey*. IEEE Transactions on Industrial Electronics, Vol. 39, No. 5, pp. 410-420 (1992).
- [13] Ogasawara, S., and Akagi, H.: *Analysis of Variation of Neutral Point Potential in Neutral-Point-Clamped Voltage Source PWM Inverters*. Proceedings of the 27th IEEE Industry Applications Society Annual Meeting, Toronto, Canada, Oct. 2-8, Pt. II, pp. 965-970 (1993).
- [14] McMurray, W.: *Modulation of the Chopping Frequency in DC Choppers and PWM Inverters Having Current-Hysteresis Controllers*. Record of the 14th IEEE Power Electronics Specialists Conference, Albuquerque, NM, June 6-9, pp. 295-299 (1983).
- [15] Nagy, I.: *Improved Current Controller for PWM Inverter Drives with the Background of Chaotic Dynamics*. Proceedings of the 20th IEEE International Conference on Industrial Electronics Control and Instrumentation, Bologna, Italy, Sept. 5-9, pp. 561-566 (1994).
- [16] Brod, D. M., and Novotny, D. W.: *Current Control of VSI-PWM Inverters*. Proceedings of the 19th IEEE Industry Applications Society Annual Meeting, Chicago, IL, Sept. 30- Oct. 4, pp. 418-425 (1984).
- [17] Tungpimolrut, K., Matsui, M., and Fukao, T.: *A Simple Limit Cycle Suppression Scheme for Hysteresis Current Controlled PWM VSI with Consideration of Switching Delay Time*. Proceedings of the 27th IEEE Industry Applications Society Annual Meeting, Houston, TX, Oct. 4-9, Vol. 1, pp. 1034-1041 (1992).
- [18] Phillips, C. L., and Harbor, R. D.: *Feedback Control Systems*. 2nd Ed., ISBN 0-13-313446-6, Prentice-Hall (1991).
- [19] Kolar, J. W., and Zach, F. C.: *Analysis of the Control Behavior of a Bidirectional Three-Phase PWM Rectifier System*. Record of the 4th European Conference on Power Electronics and Applications, Firenze, Italy, Sept. 3-6, Vol. 2, pp. 95-100 (1991).
- [20] Kolar, J. W., and Zach, F. C.: *Analysis of On- and Off-Line Optimized Current Controllers for PWM Converter Systems*. IEEE Transactions on Power Electronics, Vol. PE-6, No. 3, pp. 451-462 (1991).
- [21] Vlatkovic, V., Borojevic, D., and Lee, F. C.: *Soft Switching Three-Phase PWM Conversion Technology*. Proceedings of the 12th Annual Power Electronics Seminar, Blacksburg, VA, Sept. 11-13, pp. 17-22 (1994).
- [22] Mao, H., and Lee, F. C.: *Improved Zero-Voltage-Transition 3-Phase PWM Voltage Link Converters*. Proceedings of the 12th Annual Power Electronics Seminar, Blacksburg, VA, Sept. 11-13, pp. 53-61 (1994).